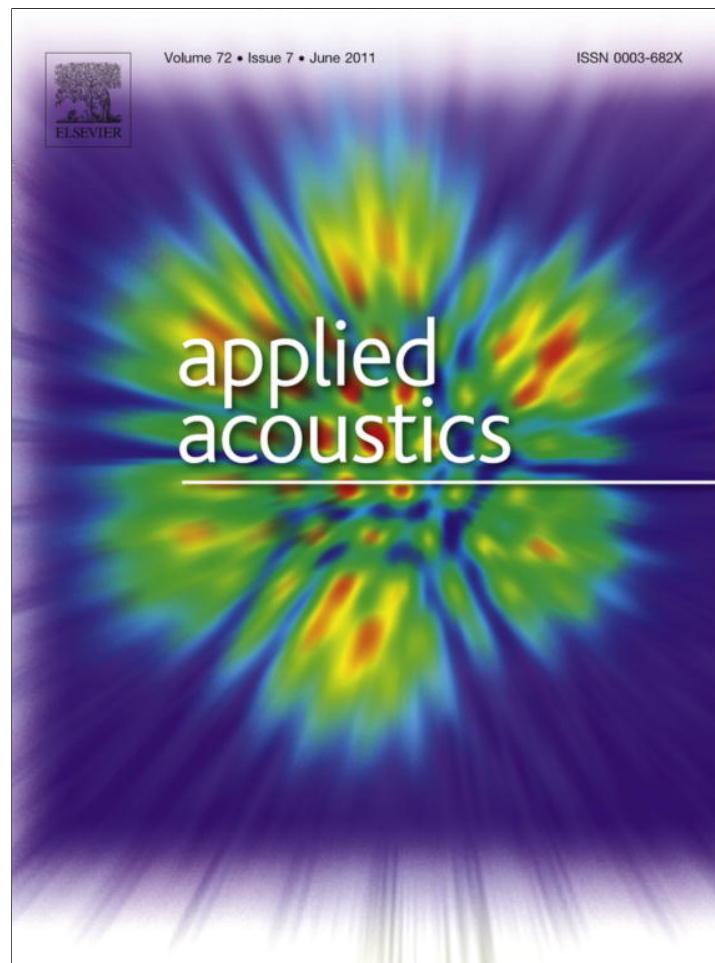


Provided for non-commercial research and education use.
Not for reproduction, distribution or commercial use.



This article appeared in a journal published by Elsevier. The attached copy is furnished to the author for internal non-commercial research and education use, including for instruction at the authors institution and sharing with colleagues.

Other uses, including reproduction and distribution, or selling or licensing copies, or posting to personal, institutional or third party websites are prohibited.

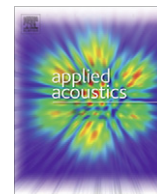
In most cases authors are permitted to post their version of the article (e.g. in Word or Tex form) to their personal website or institutional repository. Authors requiring further information regarding Elsevier's archiving and manuscript policies are encouraged to visit:

<http://www.elsevier.com/copyright>



Contents lists available at ScienceDirect

Applied Acoustics

journal homepage: www.elsevier.com/locate/apacoust

Wave propagation in stereo-lithographical (STL) bone replicas at oblique incidence

Haydar Aygün^{a,*}, Keith Attenborough^b, Walter Lauriks^c, Philip A. Rubini^d, Christian M. Langton^e^a Medical Physics, PGMI, The University of Hull, Cottingham Rd, HU6 7RX, Hull, UK^b Department of Design, Development, Environment and Materials, The Open University, Milton Keynes, MK7 6AA, UK^c Laboratorium voor Akoestiek en Thermische Fysica, Katholieke Universiteit Leuven, Celestijnenlaan 200 D, B-3001 Heverlee, Belgium^d Engineering Department, The University of Hull, Cottingham Rd, HU6 7RX, Hull, UK^e Medical Physics, Queensland University of Technology, 2 George Street, Brisbane, QLD 4001, Australia

ARTICLE INFO

Article history:

Received 24 May 2010

Received in revised form 21 January 2011

Accepted 21 January 2011

Available online 16 February 2011

Keywords:

Ultrasound

Wave propagation

Bone

Biot theory

Oblique incidence

ABSTRACT

Comparisons between predictions of a Biot-Allard model allowing for angle-dependent elasticity and angle-and-porosity dependent tortuosity and transmission data obtained at normal incidence on water-saturated replica bones are extended to oblique incidence. The model includes two parameters which are adjusted for best fit at normal incidence. Using the same parameter values, it is found that predictions of the variation of transmitted waveforms with angle through two types of bone replica are in reasonable agreement with data despite the fact that scattering is not included in the theory.

Crown Copyright © 2011 Published by Elsevier Ltd. All rights reserved.

1. Introduction

To improve the prediction of fracture risk by ultrasound it is important to understand the propagation of acoustic waves through cancellous bone. Osteoporosis is a bone disease caused by hormonal and biochemical changes. Bone essentially has two types of structure, both having the same mineralized collagen composition. Cortical bone may generally be considered to be solid; cancellous bone consists of a complex open-celled porous network of rod- and plate-shaped elements termed trabeculae. In order to understand the dependence of ultrasound propagation, in particular, upon the material and structural properties of cancellous bone, Biot-based theories have been used extensively [1–9]. Biot theory predicts two compressional waves, often referred to as ‘fast’ and ‘slow’, when the waves propagating through the solid frame of bone and marrow are in-phase and out-of-phase respectively, and a shear wave. Biot theory was developed to describe acoustic wave propagation in fluid-saturated porous elastic media at frequencies such that the wavelengths are much larger than typical microstructural dimensions [10,11]. Although its original context was geophysical testing of porous rocks, it has been used extensively to describe the wave motion in cancellous bone. It allows for an arbitrary microstructure, with separate motions considered for the solid elastic framework (bone) and

the interspersed fluid (marrow), induced by the ultrasonic wave, and also includes energy loss due to viscous friction between solid (bone) and fluid (marrow).

The anisotropic pore structure and elasticity of cancellous bone cause wave speeds and attenuation in cancellous bone to vary with angle. Aygün et al. [12] have extended previous work on the influence of anisotropic pore structure and elasticity in cancellous bone by developing an anisotropic Biot-Allard model allowing for angle-dependent elasticity, and angle-and-porosity dependent tortuosity. The extreme angle dependence of tortuosity corresponding to the parallel plate microstructure used by Hughes et al. [1] has been replaced by angle-and-porosity dependent tortuosity values based on data for slow wave transmission through air-filled stereolithography (STL) bone replicas [13]. It has been suggested that the anisotropic Biot-Allard model could be used to give further insight into the factors that have the most important influence on the angle dependency of wave speeds and attenuation in cancellous bone. Nevertheless the applicability of Biot-based theories to ultrasonic propagation in bone remains in question given the expected role of scattering which is neglected in these theories.

Most recently, Aygün et al. [14] have transmitted ultrasonic signals through water saturated stereolithographical bone replicas in the form of 57 mm cubes with microstructural dimensions that are 13 times real scale. Views of two of the stereolithographical bone replicas are shown in Fig. 1 which shows also the directions of the coordinate axes employed in subsequent analysis. The x_1 axis (perpendicular to the page) corresponds to the trabecular alignment.

* Corresponding author. Tel.: +44 1482466489.

E-mail address: haydar-aygun@hotmail.com (H. Aygün).

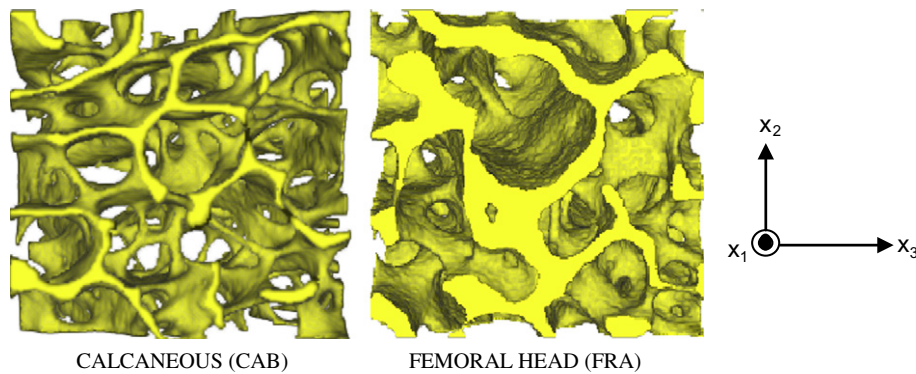


Fig. 1. Views of two stereolithographical bone replicas and the coordinate system employed for analysis.

Predictions of a modified anisotropic Biot-Allard model, which neglects scattering have been compared to measurements made at normal incidence in a water filled tank at 100 kHz and 1 MHz. Remarkably, it is found that the expected occurrence of scattering does not cause significant discrepancies between predictions and data at 100 kHz (which would be equivalent to 1.3 MHz in real bone), perhaps as a consequence of the fact that the samples behave as low pass filters. Scattering should be even more important at 1 MHz (equivalent to 13 MHz in real bone) where the fast and slow wavelengths are 3 mm and 1.5 mm respectively. Nevertheless the modified Biot-Allard theory is found to predict the observed simple relationship between incident and transmitted waveforms at 1 MHz.

The aim of this paper is to investigate ultrasonic wave transmission in water-saturated bone replicas at 1 MHz as a function of angle. The predictions of the anisotropic Biot-Allard model allowing for angle-dependent elasticity and angle-and-porosity dependent tortuosity have been compared with measurements made in a fluid (water) filled tank at 1 MHz.

2. Theory

A rigid porous sample of length L is subjected to an ultrasonic wave in fluid (water), P^i . Part of ultrasonic wave is reflected back into the fluid, P^r , while other part is transmitted through the sample, P^t . Fella et al. [5] have presented an analytical model based on the Biot's theory modified by Johnson et al. [15] to describe the viscous interaction between fluid and a porous elastic structure. The Fourier transform of the transmitted field is given by Fella et al. [5] as:

$$P_3(x, \omega) = T(\omega) \exp\left(-j\omega \frac{(x-L)}{c_0}\right) \varphi(\omega), \quad x \geq L \quad (1)$$

where $\varphi(\omega)$ is the Fourier transform of the incident field ($P^i(t)$), $T(\omega)$ is the Fourier transform of the transmission kernel, ω is the angular frequency of motion, c_0 is the speed of sound in fluid, and L is the thickness of the material. More detailed considerations of the transformed field and the transmission coefficient $T(\omega)$ can be found in the paper by Fella et al. [5].

Aygün et al. [12] have introduced a transverse anisotropy into the Biot-Allard model by allowing for an angle-and-porosity dependent tortuosity in addition to an angle-dependent elasticity. The proposed heuristic form for the porosity- and angle- dependent tortuosity is:

$$\alpha_\infty = 1 - r \left(1 - \frac{1}{\phi}\right) + k \cos^2(\theta) \quad (2)$$

where ϕ is the porosity, θ is the variable between 0° and 90° , and the parameters r and k can be considered adjustable. A range of

possible values of r and k have been found by comparing predictions of Eq. (2) for $\theta = 0^\circ$ and 90° respectively with values deduced from air-filled replicas of known porosity [13]. Values of r and k are found by solving the resulting simultaneous equations. To allow for elastic anisotropy, Williams [16] suggests that the dependence of skeletal frame modulus (Young's modulus, E_b , Bulk Modulus, K_b , and rigidity modulus, μ_b) in terms of bone volume fraction ($1-\phi$) and the Young's modulus of the solid material of the frame (E_s) are given by $E_b = E_s(1-\phi)^n$, $K_b = E_b/(1-2\nu_b)$, and $\mu_b = E_b/(1+2\nu_b)$, respectively, where ν_b is the Poisson's ratio of frame, and, according to Gibson [17], the exponent n varies from 1 to 3 depending on the angle (θ) with respect to the dominant structural orientation according to $n = n_1 \sin^2(\theta) + n_2 \cos^2(\theta)$. Values of $n_1 = 1.23$ and $n_2 = 2.35$ are chosen by Lee et al. [2] to be consistent with the work of Williams [16].

The parameters used in the predictions are listed in Table 1. The elastic moduli of the bone replicas made of resin have been taken to be equal to the elastic modulus of resin which is 6.04 GPa (DSM Somos) and is smaller than the elastic modulus of real bone which is 20 GPa (Williams [16]). Assuming that the permeability of the bone is $5 \times 10^{-9} \text{ m}^3$ (McKelvie and Palmer [9]), the permeability of bone replicas has been taken to be 169 (i.e. 13^2) times higher because the replica microstructures are larger than those of the actual bone microstructure by a factor of 13 in every direction. The assumed characteristics of the saturating fluid (water) are: density $\rho_f = 1000 \text{ kg/m}^3$, viscosity $\eta = 10^{-3} \text{ kg ms}^{-1}$, speed of sound in water $c_0 = 1490 \text{ m/s}$.

Two of the required parameters, the Poisson's ratio of the frame and the viscous characteristic length, have been adjusted for each replica to obtain the 'best-fit' at normal incidence. It has been found that the predictions are particularly sensitive to the assumed values of viscous characteristic length. The 'best-fit' characteristic length values for the two replicas cited in Table 1 are about 13 times those found for real bone which lie between 5 and 10 μm [3,5]. This is consistent with the physical scaling of the replicas.

Table 1
Default input parameters for STL bone replicas.

Parameters	Femoral Head, FRA	Calcaneus, CAB
Density of replica, ρ_s [13]	1227 kg/m ³	1171 kg/m ³
Young's modulus, E_s	6.04 GPa	6.04 GPa
Poisson's ratio of solid, ν_s	0.30	0.30
Poisson's ratio of frame, ν_b	0.40	0.34
Porosity, ϕ [13]	0.7426	0.8822
Permeability, k_0	$845 \times 10^{-9} \text{ m}^3$	$845 \times 10^{-9} \text{ m}^3$
Viscous characteristic length, Λ	60 μm	150 μm
r [12]	0.591	0.816
k (Eq. (2))	0.684	0.574

3. Measurements

Measurements have been carried out with transducers and replica bone specimens immersed in water following the procedure used by Fellah et al. [5] (see Fig. 2). Two broadband Panametrics, A303S, plane piezoelectric transducers having 1 cm diameter with 1 MHz central frequency have been used. 400 V pulses are provided by a 5058PR Panametrics pulser/receiver. Electronic interference was removed by 1000 acquisition averages. Moreover each measurement series was repeated.

Two incident (reference) signals generated by 1 MHz transducers and transmitted over corresponding path lengths in fluid (water) are shown in Figs. 3a and 4a, and their spectra are shown in Figs. 3b and 4b, respectively. These signals were used when analyzing transmission data for Calcaneous (CAB) and Femoral Head (FRA) replicas respectively.

To vary the angle of incidence, each bone replica was revolved around its central axis. For a rotation angle, θ , measured from the normal, the transmission path becomes $L \cos(\theta)$ where L is the cube dimension. Example measured variations of transmitted signals with angle and the corresponding spectra are shown in Figs. 5 and 6. The variation in the signals transmitted through the CAB replica is significant but is mainly in amplitude rather than in the structure of the waveforms whereas, in the signals transmitted through the Femoral Head replica, both amplitude and structure are influenced significantly by angle. It can be expected that shear waves should occur as well as fast and slow waves in poroelastic materials at oblique incidence. However there are no indications of separate shear wave arrivals in the measured waveforms and no allowance has been made for the occurrence of shear waves in the predictions presented later.

4. Comparisons between predictions and data

Predicted and measured transmitted waveforms in the Calcaneus and Femoral Head replicas at normal incidence are shown in Figs. 7 and 8. It seems that the shape of the incident pulse waveform is not affected much by transmission through the replicas. However it seems that only between 0.5% and 4% of the amplitude of incident wave is transmitted through bone replicas at 1 MHz. Most of the incident ultrasonic wave is reflected back into the water. Predictions of the waveforms transmitted through Calcaneus and Femoral Head replicas at four oblique angles are compared with the data in Figs. 9 and 10. Generally measured and predicted transmitted waveforms through the CAB bone replica

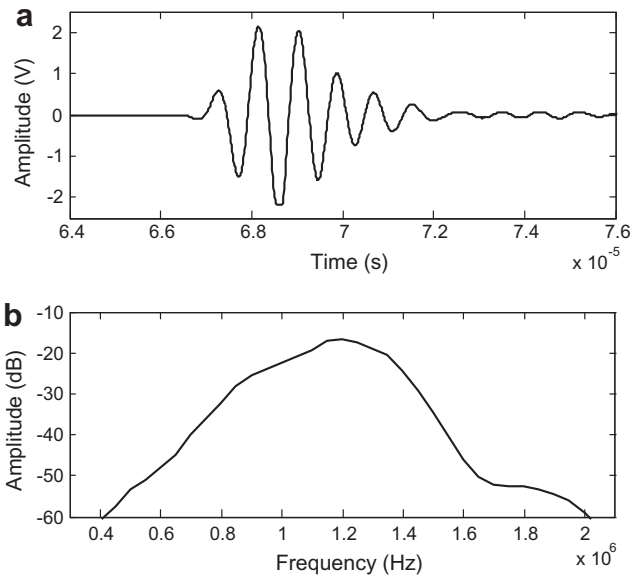


Fig. 3. (a) Incident signal for CAB versus time, and (b) its spectrum versus frequency at 1 MHz.

(Fig. 9) are similar except for the initial parts of the transmitted waveforms which can be identified as the fast wave arrivals. The subsequent major parts of the transmitted waveforms can be identified as slow wave contributions. Overall the initial parts of the transmitted waveforms are not predicted as well as the later arrivals. A possible cause might be signal leakage caused by refraction from the CAB replica at higher angles and transmission paths that fall outside the receiving transducers. Nevertheless it does not seem likely that the drop in the magnitude of the fast wave in Fig. 10 at 25° is due to signal leakage, since the initial waveform amplitude is higher at 29°. Moreover the prediction of the initial waveform at the higher angle is in better agreement with data.

The predicted arrival time of the ultrasonic waves changes when the angle of propagation is varied as a consequence of the angle dependence of tortuosity through Eq. (2).

5. Concluding remarks

Predictions of a modified anisotropic Biot-Allard theory have been compared with measurements of pulses centred on 1 MHz

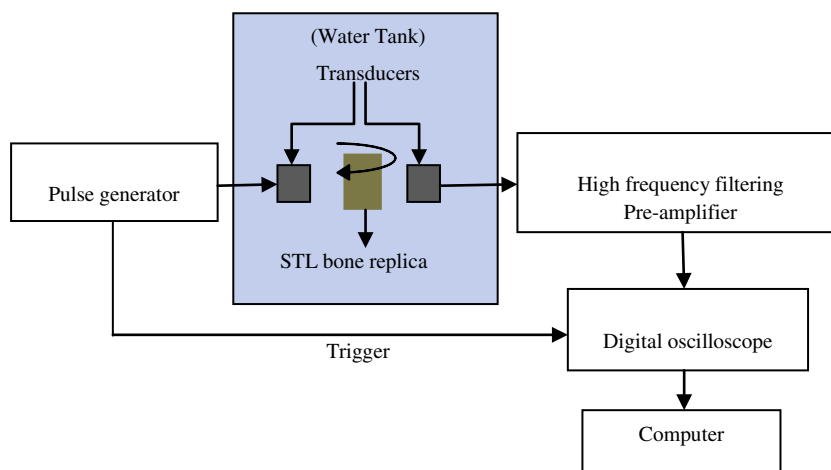


Fig. 2. Experimental setup for ultrasonic measurements.

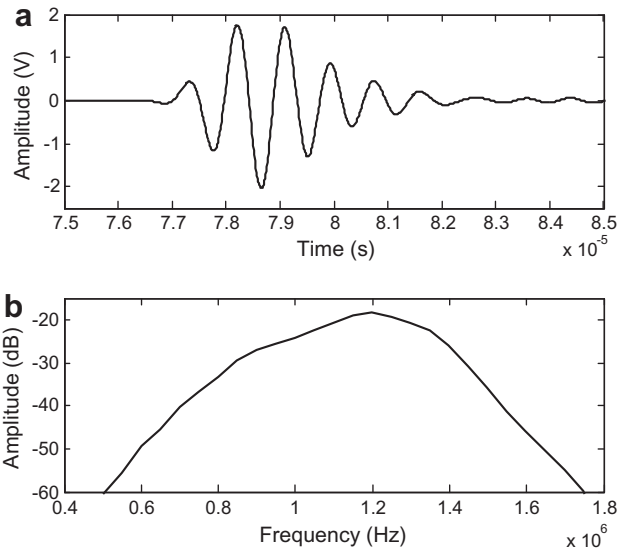


Fig. 4. (a) Incident signal for FRA versus time, and (b) its spectrum versus frequency at 1 MHz.

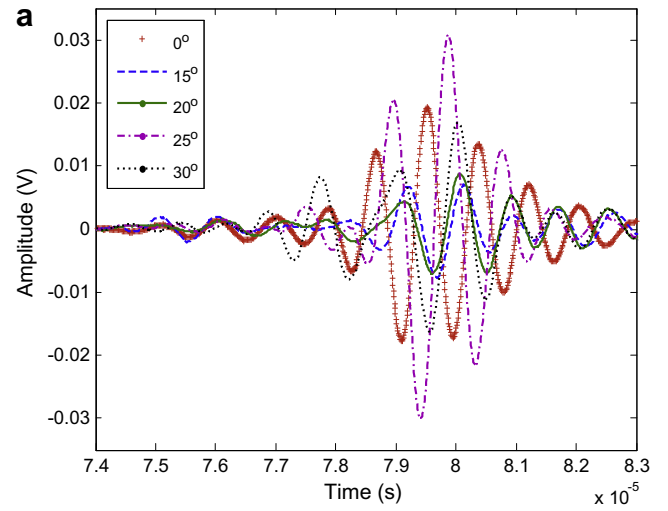


Fig. 5. (a) Measured transmitted waveforms through CAB bone replica versus time at 0°, 10°, 12°, 20°, and 29°, and (b) the corresponding spectra.

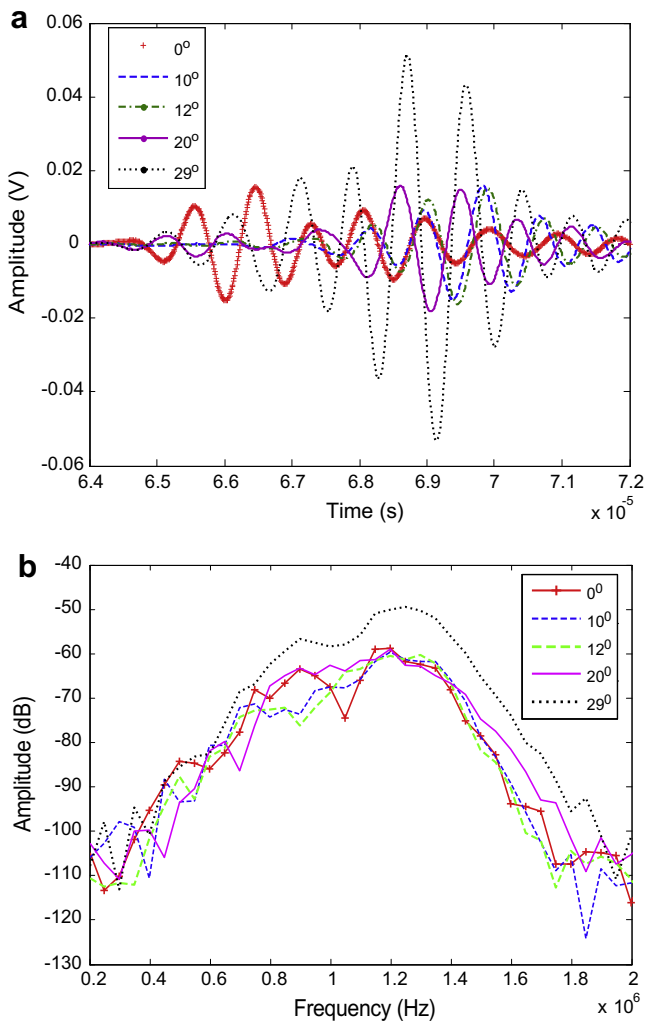


Fig. 6. (a) Measured transmitted waveforms through FRA bone replica versus time at 0°, 15°, 20°, 25°, and 30°, and (b) the corresponding spectra.

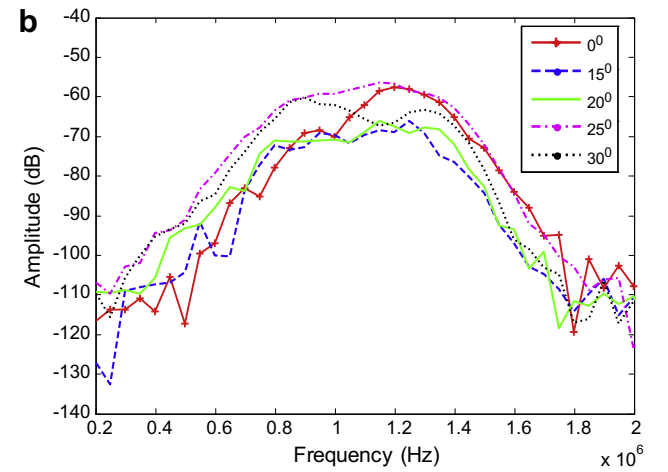


Fig. 7. Measured and predicted transmitted waveforms through Calcaneus bone replica versus time at 0°.

transmitted at normal and oblique angles through water saturated stereo-lithographical (STL) bone replicas which are thirteen times larger than the original bone samples. Use of values of two

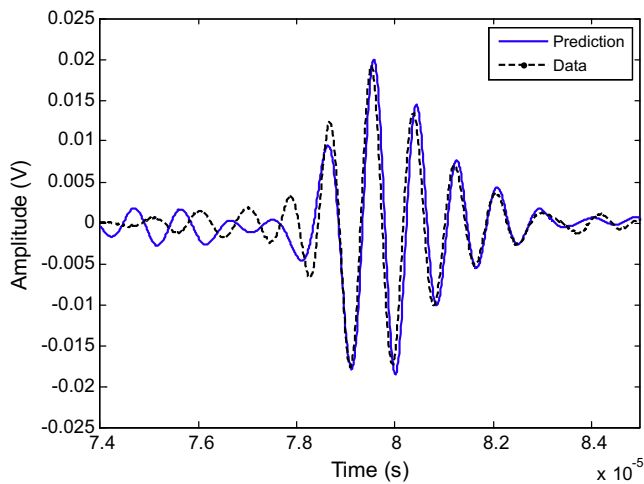


Fig. 8. Measured and predicted transmitted waveforms through FRA bone replica versus time at 0°.

parameters adjusted for best fit at normal incidence enable reasonable agreement with data obtained at oblique angles also. The predictions and data show significant agreement despite the expected role of scattering. On the other hand, the explicit inclusion of scattering might have avoided the need for adjustable parameters.

The likely ranges of validity for Biot modelling approaches can be discussed in terms of the ratio ($\epsilon = l/L$) of a characteristic inhomogeneity size (l) and the reduced sound wavelength $L = \lambda/2\pi$ (λ). Scattering is likely to be significant for values of ϵ greater than 1 whereas the Biot theory was derived for values of ϵ that are significantly less than 1. At 1 MHz the fast and slow wavelengths are 3 mm and 1.5 mm respectively. For the fast waves the values of the ratios, ϵ , in FRA and CAB replicas are 0.1257 and 0.3142 respectively, and for the slow waves the values are 0.2513 and 0.6283. These indicate clearly that scattering should be significant, so the agreement between Biot-based predictions and data at 1 MHz is rather surprising.

Recently Boutin [18] has discussed a general multiple-scale approach that allows for scattering and visco-thermal effects in a rigid-porous medium and has considered a specific application to a

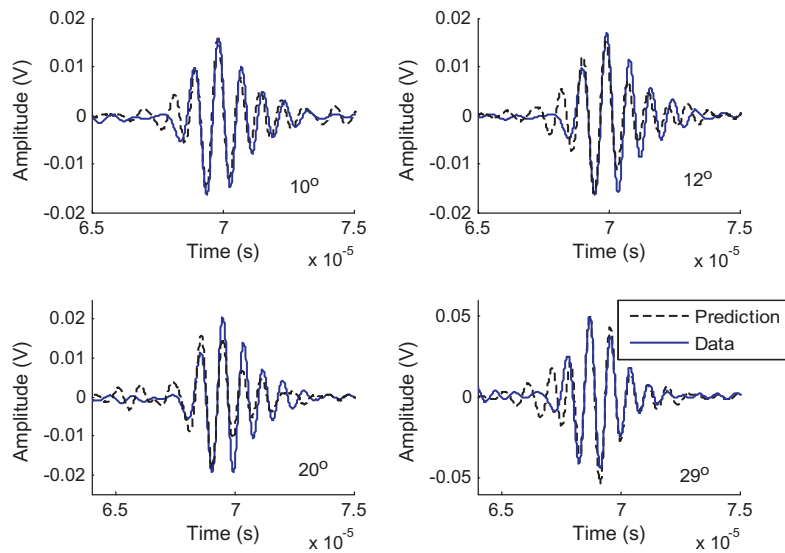


Fig. 9. Measured and predicted transmitted waveforms through CAB bone replica versus time at 10°, 12°, 20°, and 29°.

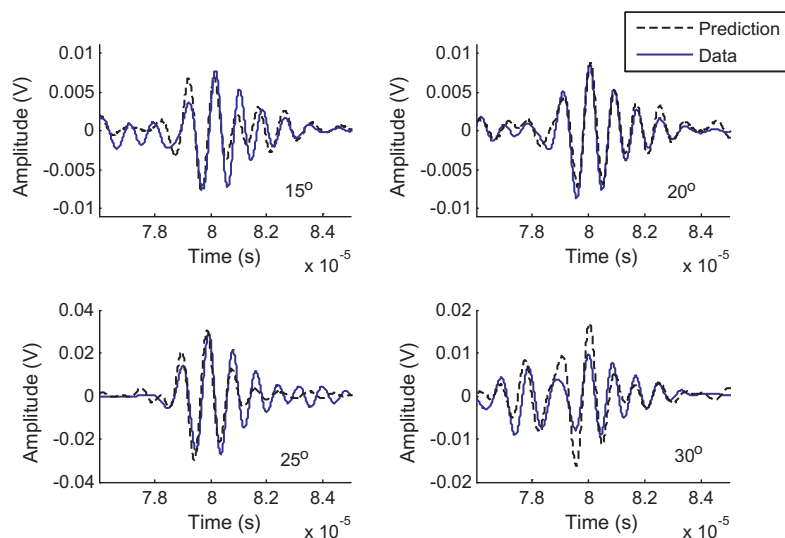


Fig. 10. Measured and predicted transmitted waveforms through FRA bone replica at 15°, 20°, 25°, and 30°.

parallel plate medium. However, the development of model capable of covering both viscous and scattering regimes and applicable to an anisotropic poroelastic medium remains a formidable challenge. Nevertheless the apparent success of the modified Biot–Allard model using only two adjustable parameters suggests that, as a next step, it might be worth considering the development of Biot–based Finite Element Models (FEM) for cancellous bone. This would enable modelling of complete bone structures which would be more appropriate to the context of clinical monitoring. Such models of the acoustical properties of complex arrangements of anisotropic porous and elastic media are used increasingly in engineering studies, for example those related to the acoustical design of vehicle interiors [19–22].

Acknowledgements

This work has been supported by Leverhulme Grant: F/00 181/N which provided for collaboration with the Laboratory of Acoustics and Thermal Physics at Leuven where the data reported here were obtained. The authors would like to dedicate this paper to the memory of Prof. Walter Lauriks who passed away prematurely while this paper was being written.

References

- [1] Hughes ER, Leighton TG, White PR, Petley GW. Investigation of an anisotropic tortuosity in a Biot model of ultrasonic propagation in cancellous bone. *J Acoust Soc Am* 2007;121:568–74.
- [2] Lee KI, Choi MJ. Phase velocity and normalized broadband ultrasonic attenuation in Polyacetal cuboid bone-mimicking phantoms. *J Acoust Soc Am* 2007;121(6):EL263–9.
- [3] Sebaa N, Fellah Z, Fellah M, Ogam E, Wirgin A, Mitri F, et al. Ultrasonic characterisation of human cancellous bone using the Biot theory: inverse problem. *J Acoust Soc Am* 2006;120:1816–24.
- [4] Lee KI, Yoon SW. Comparison of acoustic characteristics predicted by Biot's theory and the modified Biot–Attenborough model in cancellous bone. *J Biomech* 2006;39:364–8.
- [5] Fellah ZEA, Chapelon JY, Berger S, Lauriks W, Depollier C. Ultrasonic wave propagation in human cancellous bone: application of Biot theory. *J Acoust Soc Am* 2004;116:61–73.
- [6] Lee KI, Roh H-S, Yoon SW. Acoustic wave propagation in bovine cancellous bone: application of the modified Biot–Attenborough model. *J Acoust Soc Am* 2003;114:2284–93.
- [7] Hughes ER, Leighton TG, Petley GW, White PR. Ultrasonic propagation in cancellous bone: a new stratified model. *Ultrasound Med Biol* 1999;25:811–21.
- [8] Hosokawa A, Otani T. Ultrasonic wave propagation in bovine cancellous bone. *J Acoust Soc Am* 1997;101:558–62.
- [9] McKelvie ML, Palmer SB. The interaction of ultrasound with cancellous bone. *Phys Med Biol* 1991;36:1331–40.
- [10] Biot MA. Theory of propagation of elastic waves in a fluid saturated porous solid, I Low frequency range. *J Acoust Soc Am* 1956;28:168–1178.
- [11] Biot MA. Theory of propagation of elastic waves in a fluid saturated porous solid, II High frequency range. *J Acoust Soc Am* 1956;28:179–91.
- [12] Aygün H, Attenborough K, Postema M, Lauriks W, Langton CM. Predictions of angle dependent tortuosity and elasticity effects on sound propagation in cancellous bone. *J Acoust Soc Am* 2009;126(6):3286–90.
- [13] Attenborough K, Qin Q, Fagan MJ, Shin H-C, Langton CM. Measurements of tortuosity in stereolithographical bone replicas using audio-frequency pulses. *J Acoust Soc Am* 2005;118:2779–82.
- [14] Aygün H, Attenborough K, Postema M, Lauriks W, Langton CM. Ultrasonic wave propagation in Stereolithographical bone replicas. *J Acoust Soc Am* 2010;127(6):3781–9.
- [15] Johnson DL, Koplik J, Dashen R. Theory of dynamic permeability and tortuosity in fluid-saturated porous media. *J Fluid Mech* 1987;176:379–402.
- [16] Williams JL. Ultrasonic wave propagation in cancellous and cortical bone: predictions of some experimental results by Biot's theory. *J Acoust Soc Am* 1992;92:1106–12.
- [17] Gibson LJ. The mechanical behaviour of cancellous bone. *J Biomech* 1985;18:317–28.
- [18] Boutin C. Rayleigh scattering of acoustic waves in rigid porous media. *J Acoust Soc Am* 2007;122(4):1888–905.
- [19] Panneton R, Atalla N. An efficient scheme for solving the three-dimensional poroelasticity problem in acoustics. *J Acoust Soc Am* 1998;101(6):3287–98.
- [20] Hörlin NE, Nordström M, Göransson P. A 3-D hierarchical FE formulation of Biot's equations for elastoacoustic modeling of porous media. *J Sound Vib* 2001;254(4):633–52.
- [21] Gorog S, Panneton R, Atalla N. Mixed displacement–pressure formulation for acoustic anisotropic open porous media. *J Appl Phys* 1997;82(9):4192–6.
- [22] Atalla N, Panneton R, Deberque P. A mixed displacement–pressure formulation for poroelastic materials. *J Acoust Soc Am* 1997;104(3):1444–52.